Journal of Molecular Liquids 407 (2024) 125193

Contents lists available at ScienceDirect

Journal of Molecular Liquids

journal homepage: www.elsevier.com/locate/molliq

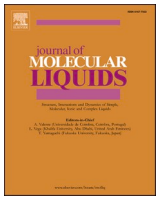

Study of self-organization and structural phase transitions in water /AOT / isopropyl myristate biocompatible system

N.V. Sautina [a,*], O.I. Gnezdilov [b], A.T. Gubaidullin [c], Yu.G. Galyametdinov [a]

[a] Kazan National Research Technological University, 68 Karl Marx Street, Kazan 420015, Russian Federation
[b] Kazan Federal University, 18 Kremlin Street, Kazan 420008, Russian Federation
[c] Arbuzov Institute of Organic and Physical Chemistry, FRC Kazan Scientific Center of RAS, 8 Arbuzov street, Kazan 420088, Russian Federation

ARTICLE INFO

Keywords:
Microemulsion
Liquid crystals
Structural phase transitions
self-diffusion NMR
Drug delivery

ABSTRACT

This work reports preparation and characterization of biocompatible sodium bis(2-ethylhexyl) sulfosuccinate (AOT) / water/ isopropyl myristate (IPM) systems. We studied their ability to form various self-organized structures such as microemulsions and liquid crystal templates for producing nanoparticles such as drug delivery vehicles, which play an important role in delivery of various substances. We determined concentration and temperature conditions that allow for forming various structures in this system and characterized the structural phase transition from the microemulsion to liquid crystalline phase, which is important for delivery of bioactive compounds. The parameters of the liquid crystalline phase of the water/AOT/isopropyl myristate system were calculated for the first time in this work. The sizes of microemulsion droplets were determined. To describe molecular motions in the studied microemulsion, self-diffusion coefficients of each component were measured. The values of relative diffusion coefficients demonstrated that reverse microemulsions were observed at AOT concentrations up to 60 % wt. Further increase in surfactant concentration slows down their molecular mobility and results in formation of aggregates with a bimodal size distribution and a subsequent formation of the hexagonal liquid crystalline phase. Geometry of the mesophase and its structure were investigated by X-ray diffraction. The respective phase diagram was plotted and analyzed using the data of polarized light microscopy, dynamic light scattering, and NMR self-diffusion. In this diagram, the areas corresponding to the microemulsion, the liquid crystal phase, and the structural phase transition were identified.

The study of the structural phase transition from the microemulsion to liquid crystal will offer a predictive power for characterizing incorporation of drugs and controlling their delivery to target cells. A deeper understanding of the structural changes is necessary to clearly determine the conditions of drug delivery.

1. Introduction

Self-assembled water/surfactant/oil systems are widely used for delivering pharmaceuticals and biologically active substances [1–8]. Microemulsions (ME) attracted much attention among the existing delivery systems. At the same time, knowledge of the type and structure of a microemulsion is of great importance for understanding the behavior of substances, which are introduced into them [9]. Another application of microemulsions is synthesis of nanoparticles allowing to control their shape and size [10,11]. Lyotropic liquid crystals (LCs) with cubic and hexagonal structures are promising substances for developing new delivery systems [12,13]. To control the release of incorporated molecules into the target cells, it is necessary to know the details of structural phase transitions, as well as mechanisms that influence the dimensional characteristics and dynamics of inter-particle interactions in such systems [14,15]. Knowledge of the structural changes during a microemulsion – liquid crystal transition is need to clearly define the conditions for the delivery of the substance.

One of the most important methods for characterizing the structure of such systems is NMR self-diffusion, which provides information about association processes, shapes and sizes of surfactant associates, and molecular dynamics of soft matter [16]. This technique is predominantly used to investigate the impact of guest molecules on dimensional characteristics of ME. In work [15], for example, the authors studied localization of the $[Ru(bpy)_3]^{2+}$ complex in a water/AOT/octane microemulsion and reported changes in the dimensions of ME and

* Corresponding author.
E-mail address: n.sautina@mail.ru (N.V. Sautina).

https://doi.org/10.1016/j.molliq.2024.125193
Received 16 February 2024; Received in revised form 17 May 2024; Accepted 3 June 2024
Available online 5 June 2024

duration of relaxation. The authors of [17] studied the impact of cyclosporine on the structure of the water / AOT / Tween 85 / isopropyl myristate system. They found that this system is represented by a bicontinuous microemulsion.

However, substances are most often released due to structural phase transitions in a system such as transformations from reverse microemulsions to liquid crystals occurring in an aqueous medium with dilution while entering the human body. It results in a durable effect of a drug due to its slow diffusion in LC [18]. At the same time, the phase diagram assumes that various structures can form and offer different patterns of release rates [19].

There is a limited number of works that study phase transitions in a concentration range of such components [20–22]. The work [20] characterized the phase behavior of the ternary system represented by unsaturated monoglycerides (UMG) DL-α-tocopheryl acetate, and water. In excess water conditions, a progressive addition of DL-α-tocopheryl acetate to a binary UMG mixture resulted in the following sequence of phases: reversed bicontinuous cubic phase, reversed hexagonal (H_{II}) phase, and reversed microemulsion. Petri et. all [21] studied the mechanisms of the photoinduced phase transitions in four different three-component systems C_iE_4 / alkane (i) with n = 8, 10, 12, 14; cyclohexane / water. The paper discussed the influence of the length of hydrocarbon chains on the transition from the microemulsion phase to the liquid crystalline phase. Nakamura et al. [22] studied the phase transition from the lamellar LC phase to ME initiated by decreasing the surfactant content in the water / sucrose monododecanoate / hexanol / decane system at the same mass content of water and decane. The data of small-angle X-ray scattering revealed a gradual increase in the interlayer distance in the liquid crystal phase upon addition of water and oil as well as localization of hexanol molecules in the lamellar LC phase.

Previously, we studied structural phase transitions in the water / lecithin / propylene glycol / vaseline oil system. According to dynamic light scattering (DLS), small-angle X-ray diffraction, and polarization optical microscopy (POM) data, we revealed changes both in the type of molecular packing and the nature of the in-phase distribution of the particles [23].

In this paper, we used NMR self-diffusion to investigate molecular level association, self-assembly, and restructuring processes in the supramolecular structure of the AOT / water / isopropyl myristate system.

2. Materials and methods

2.1. Chemicals and reagents

Sodium bis(2-ethylhexyl) sulfosuccinate (AOT, 99 %), was purchased from Sigma Aldrich, isopropyl myristate (IPM, 98 %) was purchased from Alfa Aesar. All the chemicals were used without further purification. The chemical structure of AOT (HLB = 10.5) imparts a well-balanced hydrophilic-lipophilic property. This unique feature allows the formation of alcohol-free reverse microemulsions in nonaqueous and aqueous media without any co-surfactant.

2.2. Preparation of the reverse microemulsion

For phase studies, AOT solutions in isopropyl myristate at different concentrations were taken in several stoppered test tubes and placed into a water bath at the constant temperature of 60 °C. A calculated amount of distilled water was added to each sample under constant stirring conditions.

The data for the pseudo-ternary phase diagram of the ME region were obtained by performing slow titration of a given blend of surfactant and oil with water. The titrated mixture was continuously stirred at room temperature and the ME region was identified as a transparent, low viscous and isotropic mixture. All the selected samples remained stable over a period of several months.

2.3. Self-diffusion NMR

Self-diffusion coefficients (SDCs) of the samples were measured by a Bruker AVANCE 400 NMR−spectrometer using a pulsed magnetic field gradient (G) of up to 0.53 T m^{-1}. All the measurements were carried out at 25 °C. To obtain diffusion decays, a standard diffSte pulse sequence was used. The duration of the gradient pulse was 1 ms, the diffusion time varied from 65 to 85 ms, the number of points along the gradient was 40, the maximum value of the gradient was 26 T / m, the number of accumulations was selected from 16 to 64, the time between accumulations was 5 s. In complex multiphase systems, the dependence of the amplitude of the stimulated echo on the experimental parameters satisfies the following relation:

$$A(\tau,\tau_1,t_d,q^2)=\frac{A_0}{2}\sum_i p_i\exp\left(-\frac{2\tau}{T_{2i}}-\frac{\tau_1}{T_{1i}}-q^2\left(t_d-\frac{\delta}{3}\right)D_i\right) \quad (1)$$

where A_0 is the initial amplitude of the NMR signal, $q^2=\gamma^2g^2\delta^2$ is the wave vector, γ is the gyromagnetic ratio for protons, g is the amplitude, δ is the duration of the gradient pulse, t_D is the diffusion time, p_i is the relative fraction of diffusing particles with spin–spin times T_{2i} and spin − lattice relaxation T_{1i} and the diffusion coefficient D_i, τ and τ_1 are the time intervals between the first and second, second and third radio frequency pulses in the stimulated echo sequence. The values of the self-diffusion coefficients D_i and the relative fractions of the diffusing particles p_i were determined from the analysis of diffusion attenuation.

2.4. Particle size analysis and zeta potential measurements

Size characteristics and zeta potential of microemulsions were determined by dynamic light scattering measurements (DLS), using Malvern Instrument Zetasizer Nano (Worcestershire, UK). Measured autocorrelation functions were analyzed by Malvern DTS software, applying the second-order cumulant expansion methods. The effective hydrodynamic radius (R_H) was calculated according to the Einstein-Stokes equation $D = k_BT / 6\pi\eta R_H$, where D is the self-diffusion coefficient, k_B is the Boltzmann constant, T is the absolute temperature, and η is the viscosity. The viscosity value was equal to the viscosity of isopropyl myristate (5.5 mPa·s). The diffusion coefficient was measured at least three times for each sample.

2.5. Polarized optical microscopy

The synthesized systems were analyzed for transparency and homogeneity by visual observation with an Olympus BX 51 polarized light microscope equipped with the Linkam heating system. The systems were identified as microemulsions (non-birefringent), liquid crystals (birefringent), or transition systems. This method was also used to determine the type of the mesophase and the phase transition temperature. Phase transition temperatures were measured with an accuracy of ± 0.1 °C. The systems were heated from 25 to 150 ^{0}C at a rate not exceeding 5 ^{0}C min^{-1}.

2.6. X-ray powder diffraction

The X-ray phase studies were performed on a Bruker D8 Advance diffractometer equipped with a Vario attachment and a Vantec linear PSD, using CuKa1 radiation (40 kV, 40 mA) monochromated using a Johansson curved monochromator (l = 1.5406 Å). The room temperature data were collected in the reflection mode using a flat-plate sample. The samples were loaded into a standard sample holder or on a glass plate. The patterns were recorded in the 2y range between 0.8 and 501, in 0.0081 steps, with a step interval of 0.3–1.0 s. Several diffraction patterns were collected and summarized for a sample. The geometric parameters of the mesophase were calculated as follows [24,25]: the cylinder diameter in the hexagonal phase was calculated from the

interlayer distance under the assumption that the mesophase consists of infinitely long cylinders:

$$d_h = 2d\left(\frac{2\phi}{\pi\sqrt{3}}\right)^{\frac{1}{2}} \quad (2)$$

where ϕ is the volume fraction of surfactant. The unit cell parameter dp and the distance between the surfaces of the surfactant cylinders dw were calculated as follows:

$$d_p = \frac{2d}{\sqrt{3}} \quad (3)$$

$$d_w = d_p - d_h \quad (4)$$

The molecular volume of the surfactant molecules in the hexagonal phase was calculated using the following equation:

$$V_m = \frac{M \cdot \upsilon_s}{N} \quad (5)$$

where υ_s – specific volume of surfactant, M is molecular mass, N is Avogadro constant. The cross-section area A of the surfactant molecules in hexagonal phase was calculated as:

$$A = \frac{4V_m}{d_h} \quad (6)$$

2.7. Construction of pseudo-ternary phase diagrams

In order to find out the concentration range of components corresponding to the existence range of ME, a pseudo-ternary phase diagram was constructed using water titration method at an ambient temperature (25 °C) [26]. The construction of the phase diagram was done by drawing 'water dilution lines' representing an increase in water content while decreasing surfactant and oil levels. A homogeneous mixture of IPM and AOT at these certain weight ratios ranging from 95/5 to 5/95 was slowly titrated with aliquots of bidistilled water while performing moderate magnetic stirring. After being equilibrated, the mixtures were assessed visually and identified as a single phase microemulsion or two-phase mixtures. Appearance of turbidity was considered as an indication of the phase separation. Every sample that remained transparent and homogenous after vigorous vortexing was considered as belonging to the single-phase area in the phase diagram. Visually clear samples of high viscosity were additionally checked with crossed polarizers for the presence of a liquid crystalline phase.

2.8. Amino acid release study

The amino acid serine was introduced into the aqueous phase at the concentration of 1 % wt. during preparation of the systems. The release of incorporated substances by the systems was studied by equilibrium dialysis using a Franz diffusion cell across a model membrane made of a cellophane film, as described in [27]. Sampling was done at regular intervals. The receiving medium was a Ringer's solution, i.e., a multi-component physiological solution containing 8.60 g sodium chloride, 0.30 g potassium chloride, and 0.25 g calcium chloride hexahydrate (in the form of an anhydrous salt) per 1 L of solution prepared using water for injection. The concentration Caa of the released amino acid (mol/L) in the receiving medium was determined spectrophotometrically on a PerkinElmer Lambda 35 instrument. A sample of the receiving medium (2 cm^3) was taken and transferred to the spectrophotometric cell. After measurements, it was immediately returned to the acceptor chamber of the Franz cell. The experimental data were used to calculate target component concentration Caa using by the formula 7:

$$C_{aa} = \frac{A_{max}}{E_{max}} \quad (7)$$

where A_{max} is the absorbance of the amino acid solution at wavelength λ_{max} and E_{max} is the molar extinction coefficient of amino acid in water.

The amount of substance passing across the unit surface area of a membrane in time was calculated using the Eq. (8):

$$Q = \frac{C_{aa}V}{S_0} \quad (8)$$

where V is the volume of the receiving medium (20 cm^3) and S_0 is the diffusion area, which is equal to the area of the orifice of the Franz cell.

3. Results and discussion

3.1. Characterization of microemulsions

Selection of proper biodegradable components is of great importance for developing potential delivery systems. For this reason, we proposed AOT / water / IPM systems that are non-toxic and skin-compatible. In addition, IPM is also a permeation enhancer [28,29]. At the same time, microemulsions with isopropyl myristate are effective as delivery systems in the concentration range from 10 to 85 wt% [28–32]. It is effective in microemulsions for delivering 5-Fluorouracil [30], 8-Methoxsalen [31], Felodipine [32] and others drugs. The composition of the studied systems is shown in Table 1. The amount of solubilized water is expressed as the molar ratio of water to AOT (i.e. $W = [H_2O]/[AOT]$). This ratio (W) represents the number of water molecules added per molecule of AOT in solution.

These systems remained stable for over a year. Zeta potential of microemulsions varied in the range from –33.9 to –40 mV, which indicates no tendency towards flocculation [33]. Moreover, according to [34], negative zeta potential indicates that these systems will favor transport of drugs due to repulsion of microemulsion particles from similarly charged skin.

3.2. NMR self-diffusion study of microemulsion systems

To characterize mobility of molecules in the studied microemulsion, we measured diffusion coefficients of its components by analyzing behavior of the protons of water, isopropyl myristate, and AOT. Initial information on self-diffusion in the NMR method was obtained by analyzing the dependence of the diffusion damping on the parameters of the magnetic field gradient and the diffusion time. Table 2 represents the SDCs and droplet sizes according to the NMR and DLS data, respectively.

In the systems studied in this work, the SDC of a pure water solvent is two orders of magnitude higher than that for water droplets in microemulsion. Therefore, water will be the dispersion phase and the microemulsion structure will be water-in-oil in all the systems. This is also indicated by the values of electrical conductivity. According to [35], if its values are lower than those of water (5 μS/cm), then the emulsion structure is water-in-oil.

For characterizing sizes of droplets, it is possible to use the water / AOT / octane system. The best methods for studying size characteristics of such a system are dynamic light scattering [36,37], SAXS [38,39], and fluorescence correlation spectroscopy [40]. The hydrodynamic radius of particles in these systems was found to be in the range of 2.4–4.3 nm

Table 1
Composition, degree of hydration and zeta potential of the systems at 25 ^{0}C.

System	Composition (wt.%)			W	Zeta Potential (mV)
	Water	AOT	IPM		
1	0	0	100	–	–
2	10	20	70	12.4	–33.9 ± 1.35
3	10	50	40	4.9	–37.0 ± 1.48
4	10	70	20	3.5	–40.0 ± 1.6
5	10	80	10	3.1	–

Table 2
Self-diffusion coefficients (NMR self-diffusion) and droplet sizes (DLS) of the samples.

System	$D_{IPM} \cdot 10^{10}$ (m^2/s)	$D_{AOT} \cdot 10^{10}$ (m^2/s)	$D_{H2O} \cdot 10^{10}$ (m^2/s)	R_h (nm)	PDI	Conductivity (μS/cm)
1	2.12	–	–	–	–	–
2	1.66	0.07	0.31	4.3 ± 0.17	0.166 ± 0.01	–
3	0.76	0.03	0.32	2.4 ± 0.1	0.18 ± 0.01	0.7 ± 0.028
4	0.33	0.008	0.17	110.1 ± 4.4/ 412.5 ± 16.5	0.518 ± 0.02	0.9 ± 0.036
5	0.23	0.004	0.11	–	–	2.4 ± 0.096
Water	–	–	26.2	–	–	5 ± 0.2

(Table 2), which agrees with the results obtained for the systems 3 and 2. The sizes of droplets in these systems are small. Therefore, our systems can be efficient for transport applications. Fig. 1 shows size distributions of droplets in these systems.

The size of the particles decreases with an increase in the content of AOT at the constant concentration of water, which is typical for microemulsion. An increase in AOT concentration up to 60 %–70 % wt. changes the size distribution to bimodal, which can be attributed to structural changes occurring in the system. Larger sizes of the particles in sample 4 indicate changes in self-organization and the resulting growth of the droplets. However, small particles are still present in this system. In addition, samples 4 and 5 demonstrate a sharp decrease in self-diffusion coefficients, which also indicates the presence of larger particles. Also, there is in increase in conductivity of the sample 5. Higher surfactant concentrations provide larger conductivity values if the content of water is constant. In the W/ O microemulsion, the conductivity of the aqueous phase was achieved through collisions of droplets [41]. In our case, growth of droplets and changes in their shape may lead to an increase in electrical conductivity.

To correlate the self-diffusion data with the microstructure of the system, we need to calculate the relative diffusion coefficient D/D_0 of the two solvents [42,43]. These values are obtained by dividing the diffusion coefficients of water (D^{H2O}) and oil (D^{IPM}) components in the microemulsion by those in the pure water phase (D_0^{H2O}) and isopropyl myristate in the neat phase (D_0^{IPM}), respectively.

Fig. 2 shows the dependence of the relative diffusion coefficients of water and oil on the AOT content (wt. %).

As shown in [42], a more than an order of magnitude difference in the values of the relative SDCs is the evidence of discrete droplets, i.e.,

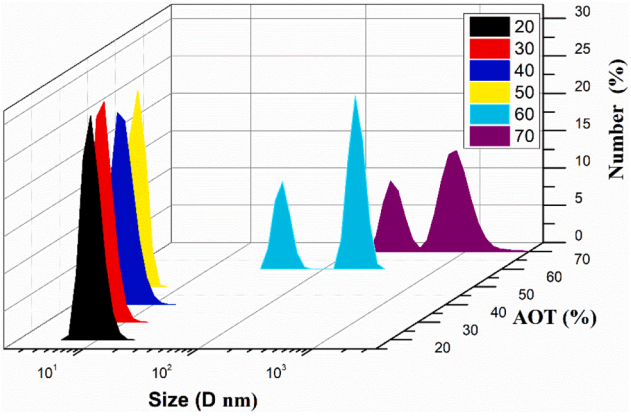

Fig. 1. Hydrodynamic diameter and size distribution of particles in water/ AOT/IPM systems at 25 °C, according to DLS.

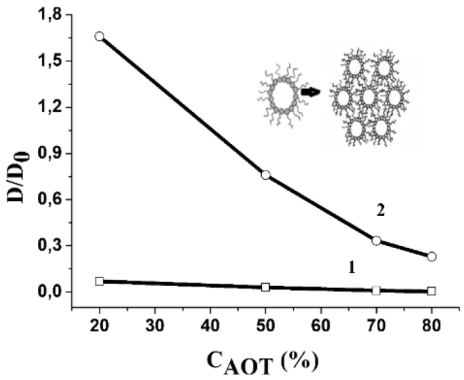

Fig. 2. Relative diffusion coefficients (D/D_0) of water (1) and oil (2) in the AOT / water / IPM systems as a function of the AOT content (wt. %).

microemulsions. In our case, such conditions are achieved with up to 60 % wt. of AOT. At the same time, the relative oil diffusion coefficient is higher than that of water. Therefore, reverse emulsions are formed at up to 60 % wt. of AOT. Further increase in the content of AOT leads to smaller differences in the relative SDCs of water and oil (Fig. 2) but also decreases the values of both coefficients. Therefore, the resulting structures are not represented by discrete droplets. We cannot confirm the presence of classical bicontinuous structures in such systems, which should provide high values of these coefficients. In the concentration range above 60 % wt. of AOT, therefore, we can assume that structural changes occur in the studied systems.

3.3. ^1H NMR spectra of the samples

To analyze changes in the structure and sizes of microemulsion droplets with an increase in AOT concentration, we recorded ^1H NMR spectral data (Fig. 3) and indexed the signals to further perform integration and obtain the diffusion decays.

The results (Table 3) reveal a considerable change in chemical shifts within spectral regions 2 and 3 with an increase in the concentration of AOT, which corresponds to the signals of the protons around the functional sulfo groups and the protons bound with the residual parts of carboxyl groups. In other spectral regions, changes in chemical shifts were insignificant. It indicates interactions of the microemulsion droplets, which results in changing the self-assembly behavior of the system.

The analysis of the results allows for a quantitative description of various microstructures according to the phase diagram and identifying transitions between them. The core component of sample 2 (its composition is shown in Table 1 and spectrum 2 in Fig. 3) is isopropyl myristate. In this system, the isopropyl myristate molecules are both in free state and in the state of coupling to the microemulsion droplets. The SDC value of the water component of sample 2 is two orders of magnitude lower than that of free water, which provides evidence for absence of free water in the system. Water can only be present as a hydration shell on micellar aggregates formed by AOT and as droplets surrounded by isopropyl myristate. Therefore, sample 2 represents a microemulsion, which is also confirmed by the relevant droplet sizes.

In sample 3, isopropyl myristate and AOT are present in approximately equal amounts (Table 1 and spectrum 3 in Fig. 3). For this sample, a proportional decrease in the SDCs of isopropyl myristate and AOT are observed as compared with sample 2 (Table 2), which can be explained by an increase in viscosity. Unlike sample 2, we observe a decrease in the size of the droplets in this case. This fact may indicate that a microemulsion medium emerges at this water/AOT/isopropyl myristate ratio. This microemulsion demonstrates a narrower size distribution of molecular aggregates.

Sample 4 (spectrum 4 in Fig. 3) represents a change in the structure of microemulsions. According to the DLS data, this system exhibits a

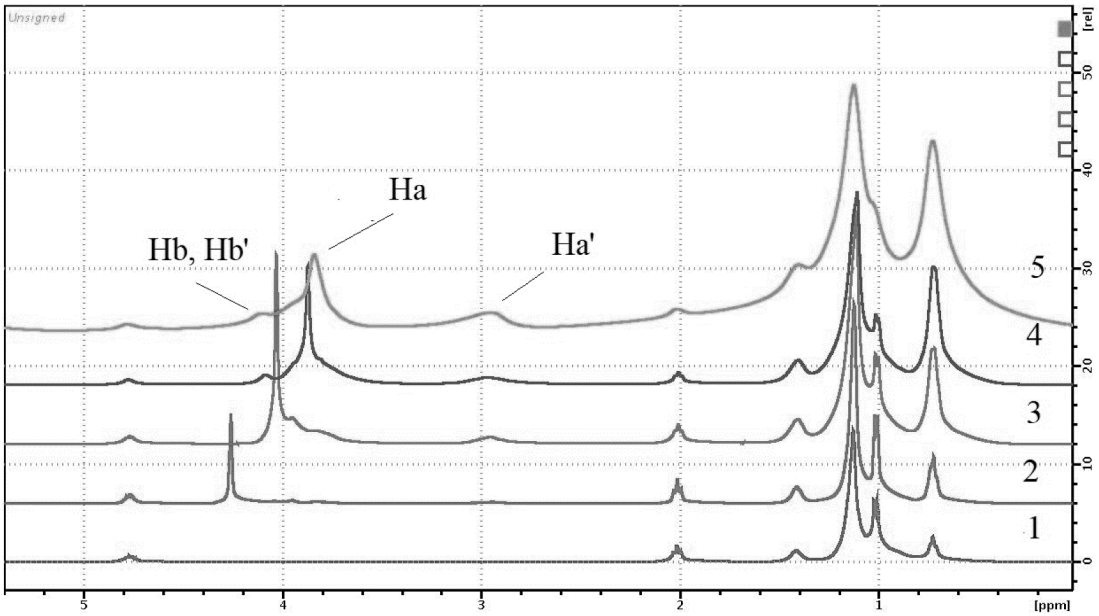

Fig. 3. [1]HNMR spectra of AOT/ water/ IPM samples. The composition of the samples is given in Table 1 NMR regions correspond to hydrogen protons shown in Fig. 4 and in Table 3.

Table 3
[1]H NMR chemical shifts and chemical shift differences of Surfactant in the AOT/water/IPM system (samples 2–5).

Functional group	δ (ppm)				Δδ(ppm)		
	δ^2	δ^3	δ^4	δ^5	$\delta^2-\delta^3$	$\delta^2-\delta^4$	$\delta^2-\delta^5$
Hb, Hb'	4.258	4.030	4.090	4.102	0.228	0.168	0.156
Ha	3.949	3.821	3.876	3.839	0.128	0.073	0.11
Ha'	2.943	2.948	2.972	2.953	−0.005	−0.029	−0.01

bimodal distribution and larger sizes of its droplets. It was found that this system includes two main fractions with the hydrodynamic radii of 110.1 and 412.5 nm, respectively. POM studies of sample 4 demonstrated certain evidences of a liquid crystalline phase, which may be attributed to microemulsion droplets balanced with some amounts of the liquid crystal. All the diffusion attenuations are characterized by slow SDC ($D = 0.0081 \cdot 10^{-10}$ m^2/s), which is approximately 4 times lower than that of sample 3. This may also indicate an increase in the size of the aggregates.

3.4. Study of liquid crystal structure

According the texture represented in Fig. 5, sample 5 has a hexagonal liquid crystalline structure.

The temperature range of the phase transition is 45–47 °C. The sample demonstrated a fan-shaped liquid crystalline texture in polarized light. According to [44], it allowed for identifying the arrangement of amphiphilic molecules in the mesophase as hexagonal.

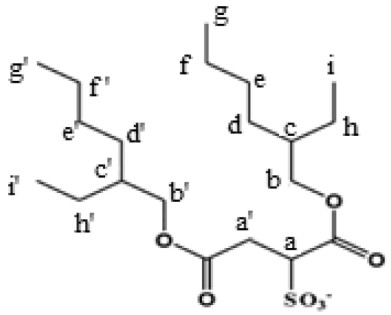

Fig. 4. Molecular structure and [1]H NMR assignment of peaks for AOT.

The type of the mesophase identified by POM was confirmed by X-ray diffraction. The diffraction diagram of the system 5 is shown in Fig. 6.

In the diffraction pattern, we observe four highly-resolved reflexes at $2\theta = 4.32^0, 7.37^0, 8.56^0$, and 11.27^0, relevant to the interlayer distances of 20.42, 11.97, 10.32, and 7.84 Å, respectively. The values of the scattering vectors q at these angles were $1:\sqrt{3}:2:\sqrt{7}$. According to [45], such values provide evidence for the existence of the 2D hexagonal liquid crystalline phase. Using the values obtained for interplanar distances, d_{100}, we computed the structural parameters characterizing the hexagonal mesophase, surfactant volume fraction (φ), elementary cell parameter (d_p), cylinder diameter (d_h), distance between cylinders (d_w), molecular volume of a surfactant molecule (V_m), and sectional area of a surfactant molecule (A) (Table 4) [24,25].

The reverse hexagonal phase formed at high surfactant concentrations. Previously [46], we found that the phase transition temperature of this system was 45-55° C. Therefore, this system maintains its structure at the temperature of human body. We also proved this by the values of the relative self-assembly coefficients. The reverse hexagonal phase is suitable for transporting a wide range of bioactive molecules and hydrophilic and lipophilic drugs [12]. The authors of [47] showed that a hexagonal mesophase provides a higher release rate of a drug as compared with a cubic one. The self-diffusion coefficient of this sample is low. According to NMR, its value is $0.0037 \cdot 10^{-10}$ m^2/s, which is virtually 20 times lower than that of sample 2 and indicates the presence of large particles in the sample, which form a hexagonal liquid crystalline structure. In [48], it was shown that the SDC value is directly proportional to the transdermal flow. Hence, we can forecast the slowed

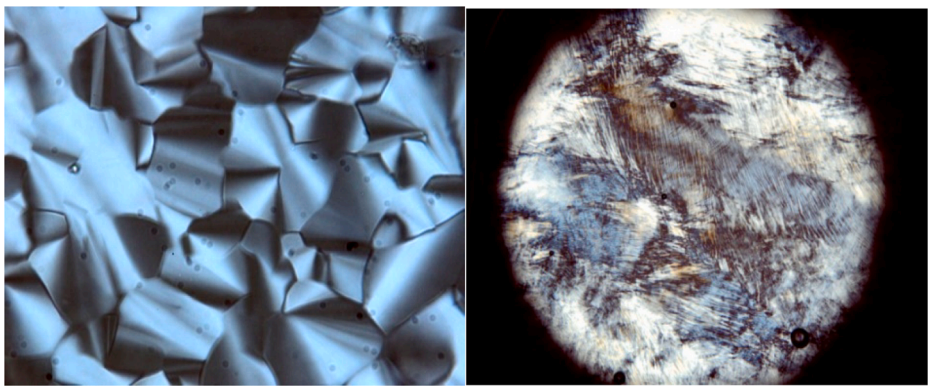

Fig. 5. Textures of sample 5, observed in polarized light (crossed polarizers, at magnification X500 and X100; T = 25 °C).

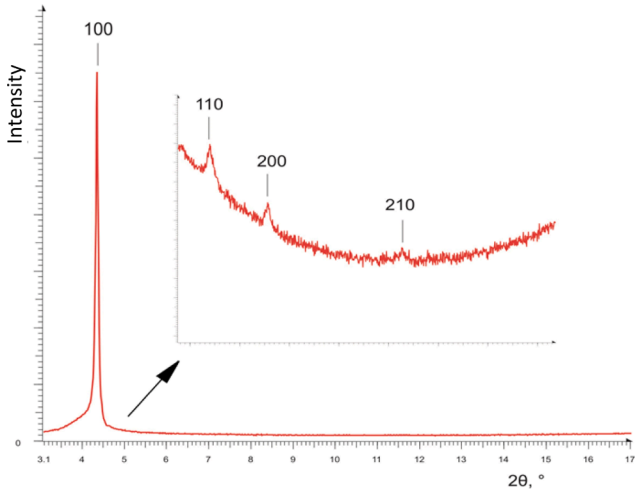

Fig. 6. Diffractogram of the System AOT/water/IPM N5.

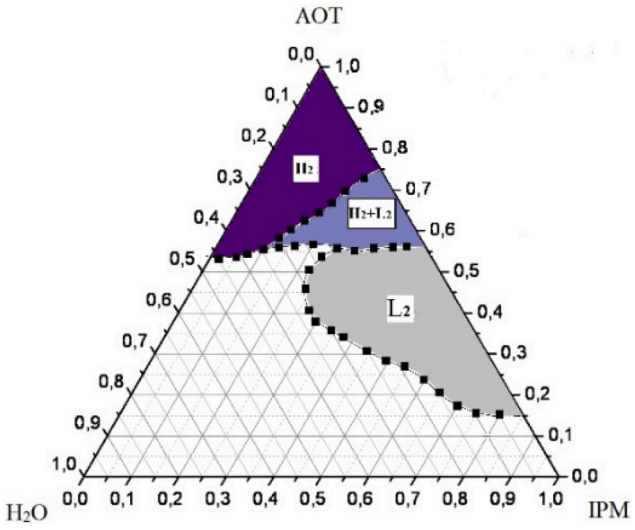

Fig. 7. Pseudo-ternary phase diagram of the AOT / water / IPM system. The phase regions are reverse ME (L_2), liquid crystal (H_2), and the transition region (L_2 + H_2). Concentrations of the components are given in wt. %.

Table 4
Geometrical parameters of the mesophase AOT / H_2O / IPM (80 / 10 / 10 (wt. %)).

Parameter	Meaning
φ	0.77
d (nm)	2.04
d_p (nm)	2.35
d_h (nm)	2.17
d_w (nm)	0.18
V_m (nm^3)	0.54
A (nm^2)	0.99

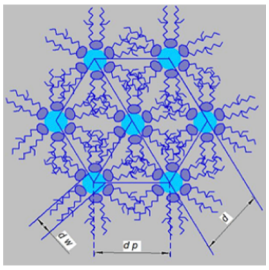

release of the active substance for system 5 that has the hexagonal liquid-crystalline structure. This releasing mechanism can be suitable for applications involving toxic pharmaceuticals, where absorption of substances by tissues must be gradual.

3.5. Plotting and characterizing the phase diagram

To study the differences in the self-assembly in this system and the microemulsion – liquid crystal transitions, we built the phase diagram of AOT / water / IPM at the constant temperature of 25 °C (Fig. 7).

In the diagram, there is large L_2 region that corresponds to reverse microemulsions. A decrease in the water content and an increase in the amount of surfactant leads to a growth in the viscosity of the solution. In polarized light, we can observe the structures typical for a hexagonal phase of liquid crystals, H_2.

3.6. Amino acid release study

Amino acids are structural elements of proteins. They participate in intermolecular interactions and represent building blocks of certain drugs [49]. To test the resulting systems for their delivery potential with respect to drugs and biologically active compounds, the release of the model amino acid serine from the microemulsion system (sample 2) and the liquid crystalline system (sample 5) was studied (Fig. 8).

The data indicate that a complete release of the amino acid from the microemulsion occurred within 180 min, while a rapid, "burst" release is observed. A complete release of amino acid from the liquid crystalline system occurred within 480 min.

We demonstrated that changing the concentration of surfactant in the system exerts a considerable impact on its self-assembly. Knowing the structural features of the system, we can synthesize various types of nanoparticles with tailored size and properties. Thus, changing the surfactant-solvent concentration ratio provides an approach to controlling the morphology of the synthesized transport system and, therefore, adjusting the release rate of the incorporated drug. Due to small sizes of microemulsions droplets, they can be used for rapid delivery of

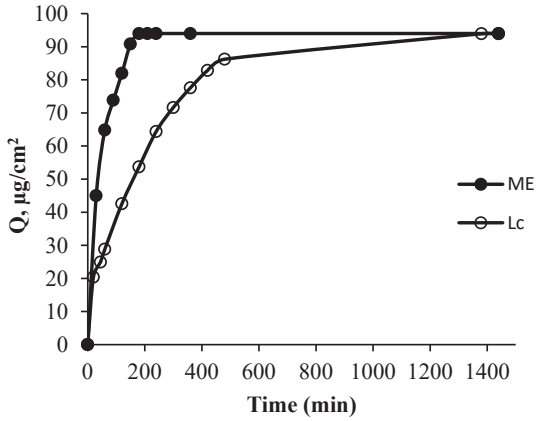

Fig. 8. Release of the amino acid serine from the systems with various self-organization: microemulsion (ME) (sample 2) and the liquid crystal (LC) (sample 5).

substances. Liquid crystal systems are needed for their slow release capabilities in toxic drugs applications when a slow absorption of a substance by tissues is required.

4. Conclusions

Biocompatible water/AOT/IPM transport systems were prepared in this work. The data obtained by the set of physicochemical methods demonstrated that drug delivery systems with different properties can potentially form in the studied mixture of components depending on their concentrations. The mobility of AOT molecules was found to considerably reduce with an increase in the surfactant concentration, due to their interactions with sulfo and carboxyl groups of AOT in neighboring microemulsion droplets. A hexagonal liquid crystalline phase was found to form in the systems with the surfactant content above 60 %. According to the experimental data, it is possible to control the size of microemulsion droplets and the interlayer distance in the mesophase, which makes it possible to use a wide range of substances in such systems for delivery of biologically active components and drugs. In addition, a possibility of a controlled transition between the phase states allows to considerably influence the conditions of intermolecular organization and, therefore, predict the delivery and release of target components into target cells.

CRediT authorship contribution statement

N.V. Sautina: Writing – original draft, Formal analysis, Data curation. **O.I. Gnezdilov:** Methodology, Investigation. **A.T. Gubaidullin:** Resources, Methodology, Investigation. **Yu.G. Galyametdinov:** Writing – original draft, Data curation, Conceptualization.

Declaration of competing interest

The authors declare the following financial interests/personal relationships which may be considered as potential competing interests: [Galyametdinov Yu.G. reports financial support was provided by Ministry of Science and Higher Education of the Russian Federation. If there are other authors, they declare that they have no known competing financial interests or personal relationships that could have appeared to influence the work reported in this paper].

Data availability

Data will be made available on request.

Acknowledgements

The manuscript was prepared using the support of Vladimir Potanin Foundation.

The work was performed using the financial support of the Ministry of Science and Higher Education of the Russian Federation within the framework of the state task for delivery of state services (performing works) of 29 December 2022, funding number 075-01508-23-00. Topic of research: “Development of Scientific Foundations for Synthesis of Novel Multifunctional Materials with a Broad Scope of Application” (FZSG-2023-0008).

Gnezdilov O.I. performed NMR measurements at the expense of a subsidy allocated to the Kazan Federal University to fulfill the state assignment in the field of scientific activity FZSM-2023-0016.

References

[1] V.P. Chavda, N.R. Gogoi, D.A. Vaghela, P.C. Baral, Parenteral microemulsions for drug delivery: advances and update, J. Drug Deliv. Sci. Technol. 89 (2023) 104991–105003, https://doi.org/10.1016/j.jddst.2023.104991.
[2] F. Grande, G. Ragno, R. Muzzalupo, M.A. Occhiuzzi, E. Mazzotta, M. De Luca, A. Garofalo, G. Ioele, Gel formulation of Nabumetone and a newly synthesized analog: microemulsion as a photoprotective topical delivery system, Pharmaceutics. 12 (2020) 423–437, https://doi.org/10.3390/pharmaceutics12050423.
[3] A. Kajbafvala, A. Salabat, Microemulsion and microemulsion gel formulation for transdermal delivery of rutin: optimization, in-vitro/ex-vivo evaluation and SPF determination, J. Dispersion Sci. Technol. (2021) 1848–1857, https://doi.org/10.1080/01932691.2021.1880928.
[4] J. Ma, X. Song, J. Luo, T. Zhao, H. Yu, B. Peng, S. Zhao, Molecular dynamics simulations insight into interfacial stability and fluidity properties of microemulsions, Langmuir 29 (2019) 8222–8232, https://doi.org/10.1021/acs.langmuir.9b02325.
[5] D.L. Manyala, M. Ghosh, S. Dalai, Novel microemulsions formulated from sodium N-Lauroyl sarcosinate as nanocarrier for encapsulation of α-tocopherol, J. Mol. Liq. 384 (2023) 122323, https://doi.org/10.1016/j.molliq.2023.122323.
[6] M.-L. Arsene, L. Raut, M. Calin, M.-L. Jecu, M. Doni, A.-M. Gurban, Versatility of reverse micelles: from biomimetic models to nano (Bio)sensor design, Processes 9 (2021) 345–387, https://doi.org/10.3390/pr9020345.
[7] Y. Poh, S. Ng, K. Ho, Formulation and characterisation of 1-ethyl-3-methylimidazolium acetate-in-oil microemulsions as the potential vehicle for drug delivery across the skin barrier, J. Mol. Liq. 273 (2019) 339–345, https://doi.org/10.1016/j.molliq.2018.10.034.
[8] W.A. Al-Otaibi, S.M. Al Motwaa, Preparation, characterization, optimization, and antibacterial evaluation of nano-emulsion incorporating essential oil extracted from teucrium polium L, J. Dispersion Sci. Technol. 44 (2021) 1–11, https://doi.org/10.1080/01932691.2021.1980000.
[9] S.P. Callender, J.A. Mathews, K. Kobernyk, S.D. Wettig, Microemulsion utilty in pharmaceuticals Implications for multi – drug delivery, Int. J. Pharma. 526 (2017) 425–442, https://doi.org/10.1016/j.ijpharm.2017.05.005.
[10] H. Wu, B. Luo, C. Gao, L. Wang, Y. Wang, Q. Zhang, Synthesis and size control of monodisperse magnesium hydroxide nanoparticles by microemulsion method, J. Dispersion Sci. Technol. 41 (2020) 1–7, https://doi.org/10.1080/01932691.2019.1594887.
[11] R.K. Sandhu, A. Kaur, P. Kaur, J.K. Rajput, Solubilization of surfactant stabilized gold nanoparticles in oil-in-water and water-in-oil microemulsions, J. Mol. Liq. 336 (2021) 116305, https://doi.org/10.1016/j.molliq.2021.116305.
[12] V.P. Chavda, S. Dyawanapelly, S. Dawre, I. Ferreira-Faria, R. Bezbaruash, N. R. Gogoy, P. Kolimi, Lyotropic liquid crystalline phase: drug delivery and biomedical application, Int. J. Pharm. 647 (2023) 123546, https://doi.org/10.1016/j.ijpharm.2023.123546.
[13] V.P. Chavda, S. Dawre, A. Pandya, L.K. Vora, Lyotrpoic liquid crystals for parenteral drug delivery, JCR. 349 (2022) 533–549, https://doi.org/10.1016/j.jconrel.2022.06.062.
[14] X. Ren, D. Svirskis, R.G. Alany, S. Zargar-Shoshtari, Z. Wu, In-situ phase transition from microemulsion to liquid crystal with the potential of prolonged parenteral drug delivery, Int. J. Pharm. 431 (2012) 130–137, https://doi.org/10.1016/j.ijpharm.2012.04.020.
[15] D.A. Binks, N. Spencer, J. Wilkie, M.M. Britton, Magnetic resonance studies of a redox probe in a reverse sodium bis(2-ethylhexyl) sulfosuccinate/octane/water microemulsion, J. Phys. Chem. B 114 (2010) 12558–12564, https://doi.org/10.1021/jp106709m.
[16] M. Fanun, W.S. Al-Diyn, Electrical conductivity and self-diffusion-NMR studies of the system: Water/sucrose laurate/ethoxylated mono-di-glyceride/isopropylmyristate, Colloids Surf. A 277 (2006) 27783–27789, https://doi.org/10.1016/j.colsurfa.2005.11.015.
[17] H. Liu, Y. Wang, Y. Lang, Bicontinuous cyclosporin a loaded water-AOT/Tween 85-Isopropylmyristate microemulsion, J. Pharm. Sci. 98 (2009) 1167–1176, https://doi.org/10.1002/jps.21485.
[18] Y. Li, A. Angelova, J. Liu, V.M. Garamus, M. Na Li, Y.G. Drechsler, A. Zou, In situ phase transition of microemulsions for parenteral injection yielding lyotropic

liquid crystalline carriers of the antitumor drug bufalin, Colloids Surf. B 173 (2019) 217–225, https://doi.org/10.1016/j.colsurfb.2018.09.023.
[19] Z. Ait-Touchente, N. Zine, N. Jaffrezic-Renault, A. Errachid, N. Lebaz, H. Fessi, A. Elaissari, Exploring the versatility of microemulsions in cutaneous drug delivery: opportunities and challenges, Nanomaterials 13 (2023) 1688, https://doi.org/10.3390/nano13101688.
[20] L. Sagalowicz, S. Guillot, S. Acquistapace, B. Schmitt, M. Maurer, A. Yaghmur, L. de Campo, M. Rouvet, M. Leser, O. Glatter, Influence of vitamin E acetate and other lipids on the phase behavior of mesophases based on unsaturated monoglycerides, Langmuir 29 (2013) 8222–8232, https://doi.org/10.1021/la305052q.
[21] M. Petri, B. Gerhard, Photo-induced phase transitions to liquid crystal phases: Influence of the chain length, Materials. 2 (2009) 1305–1322, https://doi.org/10.3390/ma2031305.
[22] N. Nakamura, T. Tagawa, K. Kihara, I. Tobita, H. Kunieda, Phase transition between microemulsion and lamellar liquid crystal, Langmuir 13 (1997) 2001–2006, https://doi.org/10.1021/la960606u.
[23] N.V. Sautina, A.T. Gubaidullin, Y.G. Galyametdinov, Phase transformations in self-organized system based on lecithin, Russian J. Appl. Chem. 90 (2017) 1789–1794, https://doi.org/10.1134/S1070427217110106.
[24] E. Alami, H. Levy, R. Zana, Alkanediyl-α,ω-bis(dimethylalkylammonium bromide) Surfactants. 2. structure of the lyotropic mesophases in the presence of water, Langmuir 9 (1993) 940–944, https://doi.org/10.1021/la00028a011.
[25] L. Mol, B. Bergenstaahl, P.E claesson forces in dimethyldodecylamine oxide - and dimethyldodecylphosphine oxide-water systems measured with an osmotic stress technique, Langmuir 9 (1993) 2926–2932, https://doi.org/10.1021/la00035a033.
[26] A.C. Sintov, H.V. Levy, S. Botner, Systemic delivery of insulin via the nasal route using a new microemulsion system: In vitro and in vivo studies, J. Control. Release 148 (2010) 168–175, https://doi.org/10.1016/j.jconrel.2010.08.004.
[27] C.H. Salamanca, A. Barrera-Ocampo, J.C. Lasso, N. Camacho, C.J. Yarce, Franz diffusion cell approach for pre-formulation characterisation of ketoprofen semi-solid dosage forms, Pharmaceutics. 10 (2018) 148–158, https://doi.org/10.3390/pharmaceutics10030148.
[28] T.N. Engelbrecht, B. Deme, B. Dobner, R.H.H. Neubert, Study of the influence of the penetration enhancer isopropyl myristate on the nanostructure of stratum corneum lipid model membranes using neutron diffraction and deuterium labelling, Skin Pharmacol. Physiol. 25 (2012) 200–207, https://doi.org/10.1159/000338538.
[29] A. Kogan, N. Garti, Microemulsions as transdermal drug delivery vehicles, Adv. Colloid Interf. Sci. 123–126 (2006) 369–385, https://doi.org/10.1016/j.cis.2006.05.014.
[30] R.R. Gupta, S.K. Jain, M. Varshney, AOT water-in-oil microemulsions as a penetration enhancer in transdermal drug delivery of 5-fluorouracil, Colloids Surf. B, Biointerfaces 41 (2005) 25–32, https://doi.org/10.1016/j.colsurfb.2004.09.008.
[31] B. Baroli, M.A. Lopez-Quintela, M.B. Delgado-Charro, A.M. Fadda, J. Blanco-Mendez, Microemulsions for topical delivery of 8-methoxsalen, J. Control. Release 69 (2000) 209–218, https://doi.org/10.1016/S0168-3659(00)00309-6.
[32] M. Trotta, S. Morel, M.R. Gasco, Effect of oil phase composition on the skin permeation of felodipine from o/w microemulsions, Die. Pharmazie 52 (1997) 50–53.
[33] C.F. Zanatta, A.M.C. de Faria Sato, F.B. de Camargo Junior, P.M.B. Gonçalves Maia Campos, P.A. Rocha-Filho, Rheological behavior, zeta potential, and accelerated stability tests of Buriti oil (Mauritia flexuosa) emulsions containing lyotropic liquid crystals, Drug Dev. Ind. Pharm. 36 (2010) 93–101, https://doi.org/10.3109/03639040903099728.
[34] J. Malakar, S.O. Sen, A.K. Nayak, K.K. Sen, Development and Evaluation of Microemulsions for transdermal delivery of insulin, ISRN Pharm. (2011) 1–7, https://doi.org/10.5402/2011/780150.
[35] Y. Alaoui, A. Fahry, Y. Rahali, N. Cherkaoui, Y. Bensouda, A. Laatiris, Formulation, optimization and characterization of ibuprofen loaded microemulsion system using D-optimal mixture design, Int. J. of Appl. Pharm. 11 (2019) 304–312, https://doi.org/10.22159/ijap.2019v11i4.33076.
[36] V.R. Vasquez, B.C. Williams, O.A. Graeve, Stability and comparative analysis of AOT/water/isooctane reverse micelle system using dynamic light scattering and molecular dynamics, J. Phys. Chem. B 115 (2011) 2979–2987, https://doi.org/10.1021/jp109202f.
[37] B. Baruah, J.M. Roden, M. Sedgwick, N.M. Correa, D.C. Crans, N.E. Levinger, When is water not water? exploring water confined in large reverse micelles using a highly charged inorganic molecular probe, J. Am. Chem. Soc. 128 (2006) 12758–12765, https://doi.org/10.1021/ja0624319.
[38] J.C. Liu, G.Z. Li, B.X. Han, Characteristics of AOT microemulsion structure: a small angle X-ray scattering study, Chin. Chem. Letts. 12 (2001) 1023–1026.
[39] S. Balakrishnan, N. Javid, H. Weingartner, R. Winter, Small-angle X-ray scattering and near-infrared vibrational spectroscopy of water confined in aerosol-OT reverse micelles, ChemPhysChem 9 (2008) 2794–2801, https://doi.org/10.1002/cphc.200800506.
[40] N. Pal, S.D. Verma, M.K. Singh, S. Sen, Fluorescence correlation spectroscopy: an efficient tool for measuring size, size-distribution and polydispersity of microemulsion droplets in solution, Analy. Chem. 83 (2011) 7736–7744, https://doi.org/10.1021/ac2012637.
[41] N. Wang, J. Wang, Y. Li, Reverse microemulsion prepared by AOT/CTAB/SDS/Tween80 for extraction of tea residues protein, J. Mol. Liq. 320 (2020) 114474, https://doi.org/10.1016/j.molliq.2020.114474.
[42] M. Fanun, Conductivity viscosity, NMR and diclofenac solubilization capacity studies of mixed nonionic surfactants microemulsions, J. Mol. Liq. 135 (2007) 5–13, https://doi.org/10.1016/j.molliq.2006.09.003.
[43] R.M. Hathout, T.J. Woodman, Application of NMR in the characterization of pharmaceutical microemulsions, J. Control. Release 161 (2012) 62–72, https://doi.org/10.1016/j.jconrel.2012.04.032.
[44] D. Demus, J. Goodby, G.W. Gray, H.-W. Spies, Handbook of liquid crystals, Wiley-VCH, Weiheim, 1998, pp. 341–392.
[45] R. Rajabalaya, M.N. Musa, N. Kifli, S.R. David, Oral and transdermal drug delivery systems: role of lipid-based lyotropic liquid crystals, Drug Des., Develop. Therapy 11 (2017) 393–406, https://doi.org/10.2147/DDDT.S103505.
[46] N.V. Sautina, Y.G. Galyametdinov, Effect of L-lysine on the phase transition temperature in a three component water/ sodium bis(2- ethylhexyl) sulfosuccinate/isopropyl myristate system, Russian J. Phys. Chem. A 93 (2019) 860–864, https://doi.org/10.1134/S003602441905025X.
[47] R. Muzzalupo, L. Tavano, F.P. Nicoletta, S. Trombino, R. Cassano, N. Picci, Liquid crystalline Pluronic 105 pharmacogels as drug delivery systems: preparation, characterization, and in vitro transdermal release, J. Drug Targ. 18 (2010) 404–411, https://doi.org/10.3109/10611860903494211.
[48] J. Mo, G. Milleret, M. Nagaraj, Liquid crystal nanoparticle for commercial drug delivery, Liq. Cryst. Rev. 5 (2017) 69–85, https://doi.org/10.1080/21680396.2017.1361874.
[49] N.G. Arutyunyan, L.R. Arutyunyan, V.V. Grigoryan, R.S. Arutyunyan, Effect of aminoacids on the critical micellization concentrationof different surfactants, Colloid J. 70 (2008) 715–717, https://doi.org/10.1134/S1061933X08050177.